SoC-Based Droop Method for Distributed Energy Storage in DC Microgrid Applications

Lu, Xiaonan; Sun, Kai; Guerrero, Josep M.; Vasquez, Juan Carlos; Huang, Lipei; Teodorescu, Remus

Published in:
Proceedings of the 21st IEEE International Symposium on Industrial Electronics (ISIE)

DOI (link to publication from Publisher):
10.1109/ISIE.2012.6237336

Publication date:
2012

Document Version
Early version, also known as pre-print

This document is a preprint of the final paper: Xiaonan Lu; Kai Sun; Guerrero, J.M.; Vasquez, J.C.; Lipei Huang; Teodorescu, R.; , "SoC-based droop method for distributed energy storage in DC microgrid applications," Industrial Electronics (ISIE), 2012 IEEE International Symposium on , vol., no., pp.1640-1645, 28-31 May 2012. doi: 10.1109/ISIE.2012.6237336
URL: http://ieeexplore.ieee.org/stamp/stamp.jsp?tp=&arnumber=6237336&isnumber=6237048

SoC-Based Droop Method for Distributed Energy Storage in DC Microgrid Applications

Xiaonan Lu[1], Kai Sun[1], Josep M. Guerrero[2], Juan C. Vasquez[2], Lipei Huang[1], Remus Teodorescu[2]

1. State Key Lab of Power Systems, Department of Electrical Engineering, Tsinghua University, Beijing, China

2. Department of Energy Technology, Aalborg University, Aalborg, Denmark

Contact: joz@et.aau.dk

***Abstract*-With the progress of distributed generation nowadays, microgrid is employed to integrate different renewable energy sources into a certain area. For several kinds of renewable sources have DC outputs, DC microgrid has drawn more attention recently. Meanwhile, to deal with the uncertainty in the output of microgrid system, distributed energy storage is usually adopted. Considering that the state-of-charge (SoC) of each battery may not be the same, decentralized droop control method based on SoC is shown in this paper to reach proportional load power sharing. With this method, the battery with higher SoC supplies more load power, while the one with lower SoC supplies less load power. Different kinds of relationship between SoC and droop coefficient are selected and their performance of power sharing speed is evaluated. Small signal model of SoC-based droop method is reached to test the system stability. Theoretical analysis is validated by both simulation and experimental results.**

I. INTRODUCTION

For the rapid development of industry application and the existing problems caused by conventional fossil fuel, renewable energy as a kind of clean energy form has drawn more attention nowadays [1, 2]. With the increasing penetration of renewable energy into modern power system, the concept of Microgrid is proposed several years ago, in order to integrate numbers of renewable energy sources together into a certain area [3]. With different electricity forms, the practical microgrid can be divided into AC microgrid and DC microgrid. Since the conventional power system has AC form, more research on AC microgrid has been done. However, for kinds of renewable energy sources have DC outputs, it is much easier to connect them together in a DC microgrid [4]. Therefore, there is a heightened awareness on DC microgrid in the current research.

For the renewable energy sources are distributed connected in a microgrid, the interface converters are connected in parallel. Hence, load current sharing is a key issue in a microgrid application [4-6]. Several load sharing methods can be found in the literatures. Centralized control method is proposed in [7], where a central controller is adopted to give the current reference in each converter. Master-slave control in [8] shows a combination of one voltage-controlled converter and several current-controlled converters. The voltage-controlled converter generates the current reference for the other current-controlled converters. In [9], a method named circular-chain-control (3C) is proposed, in which the converters are cascaded connected and each converter generates the current reference for the following one. Average current control method is proposed in [10], where the current references are generated and transferred to each converter through a communication line. In the above methods, though the steady and dynamic performance of current sharing can be guaranteed, high-frequency communication is required in the system. Hence, the system redundancy is lowered down and the maintenance cost is higher. Meanwhile, high-frequency communication cannot meet the requirement of distributed characteristic. To solve the problem caused by high-frequency communication, droop method is employed to reach current sharing in microgrid applications [4, 11-12]. With droop method, decentralized control for each interface converter is achieved. At the same time, no communication or low-frequency communication is needed, which is much easier to be accomplished and higher system reliability and lower cost can be realized as a result.

To deal with the uncertainty problem in renewable energy system and enlarge system reserve capacity, distributed energy storage is required in a microgrid. For the state-of-charge (SoC) of each energy storage unit may not be exactly the same, efficient load sharing method should be developed to balance the output power in each battery, like the idea from gain-scheduling droop method [13-14]. It means that the battery with higher SoC should give more power while the one with lower SoC should give less. For this reason, different from conventional current sharing methods, which are mainly focused on the target of equal sharing, proportional load power sharing between each energy storage unit should be achieved. As aforementioned, droop control is a kind of suitable method for power sharing in microgrid application. Hence, proportional power sharing method based on droop control is proposed, which is reached by changing the droop coefficients according to the SoCs of the batteries [4]. For only conceptual solution is proposed in [4], detailed analysis and demonstration should be done for extension. At the same time, in the relationship shown in [4], the droop coefficient is inverse proportional to SoC, while no other forms between droop coefficient and SoC are discussed.

Different relationships should be analyzed to see whether the power sharing performance will be influenced or not.

In order to balance active power between distributed energy sources with different SoCs, a droop-based proportional power sharing method in a DC microgrid is proposed in this paper. Different kinds of relationship between droop coefficient and SoC are involved and the speed for load power sharing is evaluated. Small signal model of droop control system with SoC is realized to test the system stability. Theoretical analyses are demonstrated by both simulation and experimental results.

The paper is organized as follows. Section II employs different kinds of relationship between droop coefficient and SoC. The performance of power sharing speed for each relationship is evaluated. Meanwhile, the small signal model for SoC-based droop control is reached to test the stability of the system. Section III shows the simulation results. A 2×2.2 kW prototype is implemented and the experimental validation results are shown in Section IV. Finally, Section V summarizes the paper and reaches the conclusion.

II. SoC-Based Droop Control Method

Take a DC microgrid with two distributed energy storage units as an example. The control diagram of the system is shown in Fig. 1, including the characteristic of DC droop control.

The performance of load power sharing speed is demonstrated by the large scale model. To reach the corresponding system model of SoC-based droop control method, the estimation arithmetic for SoC should be achieved first. Here, the basic method based on coulomb counting is adopted, as shown below.

$$SoC_1 = SoC_1^* - \frac{1}{C_e}\int i_{dc1}dt \tag{1}$$

$$SoC_2 = SoC_2^* - \frac{1}{C_e}\int i_{dc2}dt \tag{2}$$

where i_{dc1} and i_{dc2} are the output currents of each battery, SoC_1^* and SoC_2^* are the initial values of SoC, and C_e is the battery capacity.

Omitting the power loss in the converter and suppose that the output voltages of the batteries are the same, it can be achieved that

$$p_1 = p_{in1} = V_{in} i_{dc1} \tag{3}$$

$$p_2 = p_{in2} = V_{in} i_{dc2} \tag{4}$$

where V_{in} is the input voltage of the converter, p_1 and p_2 are the output power of each converter, and p_{in1} and p_{in2} are the input power of each converter.

Combining (1) ~ (4), it yields that

$$SoC_1 = SoC_1^* - \frac{1}{C_e V_{in}}\int p_1 dt \tag{5}$$

$$SoC_2 = SoC_2^* - \frac{1}{C_e V_{in}}\int p_2 dt \tag{6}$$

Meanwhile, the droop method for DC microgrid is shown as

$$v_{dc1} = v_{dc}^* - m_1 p_{LPF1} \tag{7}$$

$$v_{dc2} = v_{dc}^* - m_2 p_{LPF2} \tag{8}$$

where v_{dc1} and v_{dc2} are the DC output values of each converter, p_{LPF1} and p_{LPF2} are the filtered output power by low-pass filters, and m_1 and m_2 are the droop coefficients.

Suppose that the converters in a DC microgrid are near each other and neglect the losses in power cable,

$$v_{dc1} = v_{dc2} = v_{dc} \tag{9}$$

where v_{dc} is the load voltage.

Hence, it is derived from (7) ~ (9) that

$$p_{LPF1} / p_{LPF2} = m_2 / m_1 \tag{10}$$

For the dynamic process of SoC is much longer than that of droop-based load power sharing method, it can be supposed that

$$p_1 / p_2 \approx p_{LPF1} / p_{LPF2} = m_2 / m_1 \tag{11}$$

It is seen from (11) that the output power of each converter can be adjusted by changing the droop coefficient. Therefore, considering different kinds of relationship between droop coefficient and SoC, the following droop method can be employed

$$m_1 = m_0 / SoC_1^n \tag{12}$$

$$m_2 = m_0 / SoC_2^n \tag{13}$$

where m_0 is an initial droop coefficient and n is the power exponent of SoC.

Conventionally, n equals to 1. Here, different values of n are selected to test the corresponding performance of power sharing speed. In (12) and (13), m_0 can be confirmed by the accepted maximum value of voltage deviation at the full load condition. To each converter, it is concluded from (7) and (8) that

$$m_0 \le \frac{\Delta V_{dc\,max} SoC_{min}}{P_{L\,max}} \tag{14}$$

where $\Delta V_{dc\,max}$ is the maximum value of DC voltage deviation, SoC_{min} is the minimum value of SoC, and P_L max is the maximum value of load power.

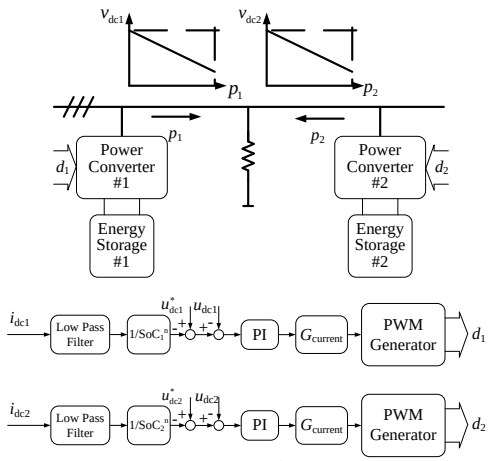

Fig. 1. Control diagram for each converter.

At the same time, as the load power is shared by the parallel converters, it is obtained that

$$p_1 + p_2 = p_L \tag{15}$$

Combining (5) ~ (6), (11) ~ (13) and (15), it is reached that

$$SoC_1 = SoC_1^* - \frac{p_L}{C_e V_{in}} \int \frac{SoC_1^n}{SoC_1^n + SoC_2^n} dt \tag{16}$$

$$SoC_2 = SoC_2^* - \frac{p_L}{C_e V_{in}} \int \frac{SoC_2^n}{SoC_1^n + SoC_2^n} dt \tag{17}$$

Combine (16) and (17) and achieve its numeric solution, the power sharing speed with different n can be tested. The parameters adopted are shown in Table I. Here, the initial values of SoC_1 and SoC_2 are 90% and 80%, respectively. In Fig. 2, the waveforms of SoC_1, SoC_2 and their difference are shown. It is seen that with larger n, SoC_1 and SoC_2 become equal with shorter dynamic process, which means that compare to the conceptual SoC-based droop method with the power exponent 1, higher load power sharing speed is realized by increasing variable n.

To test the dynamic performance of the above control system, small signal analysis is accomplished.

Perturbing (5) ~ (8), it is derived that

$$m_0 \hat{p}_{LPF1} = -nSoC_1^{n-1}(V_{dc}^* - V_{dc1}) \cdot \frac{1}{C_e V_{in} \cdot sG_{LPF}} \cdot \hat{p}_{LPF1} - SoC_1^n \hat{v}_{dc1} \tag{18}$$

$$m_0 \hat{p}_{LPF2} = -nSoC_2^{n-1}(V_{dc}^* - V_{dc2}) \cdot \frac{1}{C_e V_{in} \cdot sG_{LPF}} \cdot \hat{p}_{LPF2} - SoC_2^n \hat{v}_{dc2} \tag{19}$$

where ^ denotes the perturbed values and capital letters show the equilibrium point values. G_{LPF} is the transfer function of the low-pass filter, as shown below.

$$G_{LPF} = \frac{\omega_c}{s + \omega_c} \tag{20}$$

where ω_c is the cutting frequency of the filter.

Suppose that

$$k_{in1} = nSoC_1^{n-1}(V_{dc}^* - V_{dc1}) \cdot \frac{1}{C_e V_{in}} \tag{21}$$

$$k_{in2} = nSoC_1^{n-1}(V_{dc}^* - V_{dc2}) \cdot \frac{1}{C_e V_{in}} \tag{22}$$

So, (18) and (19) are rewritten as

$$m_0 \hat{p}_{LPF1} = -\frac{k_{in1}}{sG_{LPF}} \cdot \hat{p}_{LPF1} - SoC_1^n \hat{v}_{dc1} \tag{23}$$

$$m_0 \hat{p}_{LPF2} = -\frac{k_{in2}}{sG_{LPF}} \cdot \hat{p}_{LPF2} - SoC_2^n \hat{v}_{dc2} \tag{24}$$

On the load side, it is obtained that

$$p_L = \frac{v_{dc}^2}{R_L} \tag{25}$$

where R_L is the load resistor.

As a result, substituting (25) into (15) and taking the filtered output power into account, the result can be perturbed as

$$\hat{p}_{LPF1} + \hat{p}_{LPF2} = \frac{2V_{dc}}{G_{LPF} \cdot R_L} \hat{v}_{dc} \tag{26}$$

Meanwhile, it is achieved from (9) that

$$\hat{v}_{dc1} = \hat{v}_{dc2} = \hat{v}_{dc} \tag{27}$$

Combining (23), (24), (26) and (27), the system characteristic equation is reached as

$$A \cdot s^3 + B \cdot s^2 + C \cdot s + D = 0 \tag{28}$$

where A, B, C and D are

$$\begin{aligned}
A &= 2V_{dc} m_0^2 \omega_c^2 + 2V_{dc}(k_{in1} + k_{in2})\omega_c + 2V_{dc} k_{in1} k_{in2} \\
B &= m_0 R_L \omega_c^3 (SoC_1^n + SoC_2^n) \\
&\quad + R_L \omega_c^2 (k_{in2} SoC_1^n + k_{in1} SoC_2^n) \\
&\quad + 2V_{dc} m_0^2 \omega_c^3 + 4V_{dc} \omega_c^2 (k_{in1} + k_{in2}) \\
&\quad + 6V_{dc} k_{in1} k_{in2} \omega_c \\
C &= R_L \omega_c^3 (k_{in2} SoC_1^n + k_{in1} SoC_2^n) \\
&\quad + 2V_{dc} \omega_c^3 (k_{in1} + k_{in2}) + 6V_{dc} k_{in1} k_{in2} \omega_c^2 \\
D &= 2V_{dc} k_{in1} k_{in2} \omega_c^3
\end{aligned}$$

With the parameters shown in Table I, the system root locus can be achieved. Fig. 3 (a) shows the root locus plot with different power exponent n. It is seen that when n is changing from 2 to 9, all the poles are located at the left half of the plant and the system stability is guaranteed. The area with dominant poles is magnified, as shown in Fig. 3 (b). For the plot is symmetrical top to bottom, only the dominant poles in the top half of the plane are shown here. Fig. 4 shows the results with different SoC. It is seen that when SoC is changing from 40% to 100%, the system stability can be also guaranteed.

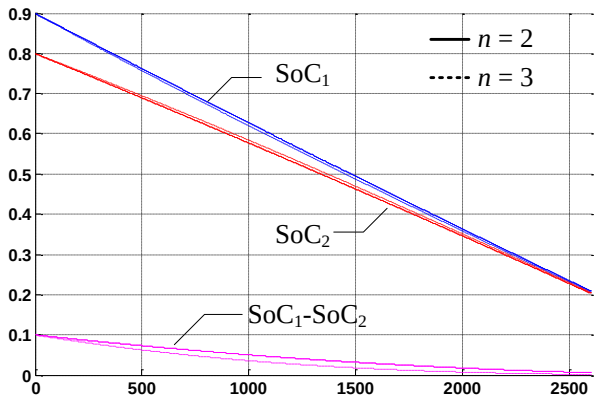

Fig. 2. Waveforms of SoC_1 and SoC_2 with different power exponent n.

TABLE I
SYSTEM PARAMETERS

Item	Symbol	Nominal Value	Unit
Initial SoC_1	SoC_1^*	90	%
Initial SoC_2	SoC_2^*	80	%
Initial Droop Coefficient	m_0	0.006	V/kW
Load Power	p_L	1.8	kW
Battery Capacity	C_e	600	Ah
Converter Input Voltage	V_{in}	100	V
DC Reference Voltage	V_{dc}^*	600	V
Cutting Frequency of LPF	ω_c	126	$rads^{-1}$
Switching Frequency	f_s	8	kHz

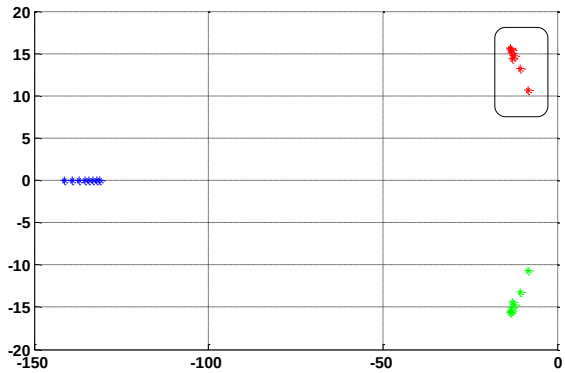

(a)

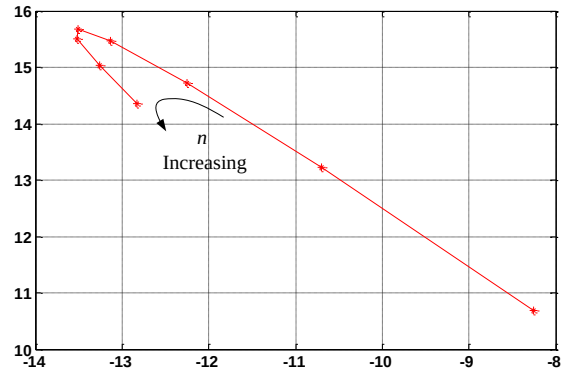

(b)

Fig. 3. Root locus plot of SoC-based droop control with different power exponent n.
(a) Plot in the whole plane. (b) Magnified result of the dominant poles.

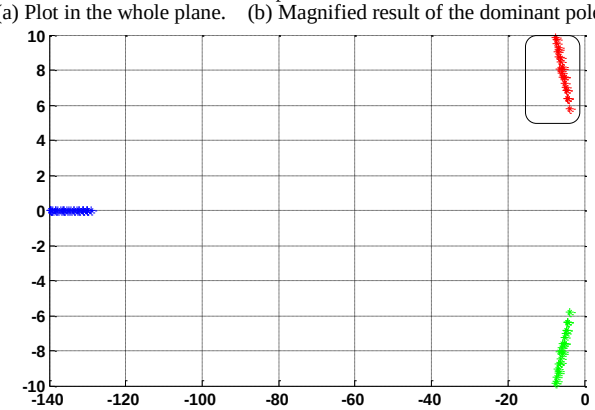

(a)

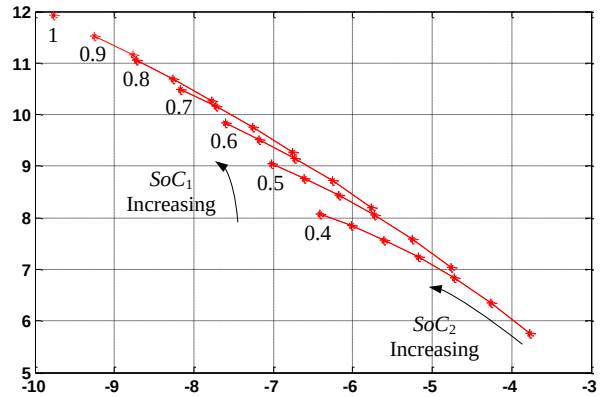

(b)

Fig.4. Root locus plot of SoC-based droop control with different SoC.
(a) Plot in the whole plane. (b) Magnified result of the dominant poles.

III. SIMULATION VALIDATION

Simulation based on Matlab/Simulink is accomplished to evaluate the performance of SoC-based droop control method. The system parameters are the same as those shown in Table I.

The proportional load power sharing by droop method is tested first. The droop coefficient m_1 is half of m_2. With different droop coefficients, the load power distribution result in the parallel converters is shown in Fig. 5. When the load resistance is changing, different output current values in each converter are shown by the data points, where the theoretical waveform is also shown for comparison. It is seen that proportional power sharing is realized by droop control with different coefficients.

At the same time, when the droop control method is adopted, DC voltage deviation is tested, as shown in Fig. 6. By selecting appropriate droop coefficient, the deviation in DC voltage can be regulated into the accepted range.

After testing the basic droop function, SoC-based droop method is tested. When the power exponent n equals to 2, the waveforms of output power in each converter are shown in Fig. 7. The initial values of SoC_1 and SoC_2 are 90% and 80%, respectively. When the system starts, the energy storage unit with larger SoC gives more power, while the one with smaller SoC gives less power. The difference between the values of active power in each converter is gradually becoming small. Similar results when n equals to 3 and 6 are shown in Fig. 8 and Fig. 9. Comparing Fig. 7 ~ Fig. 9, it is found that with larger power exponent n, the dynamic process of active power sharing is faster, which is in accordance with the theoretical analysis.

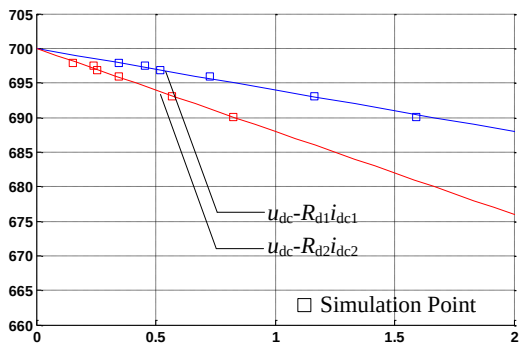

Fig.5. Results of the proportional power sharing by droop control (Simulation).

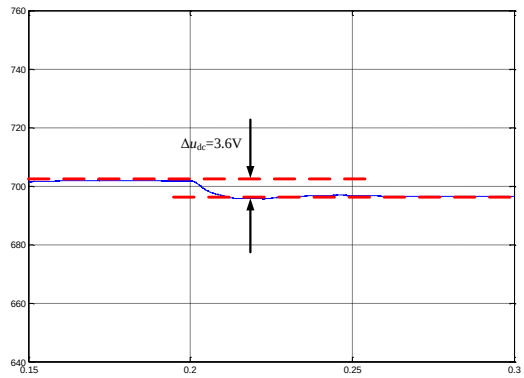

Fig.6. DC voltage deviation caused by droop control (Simulation).

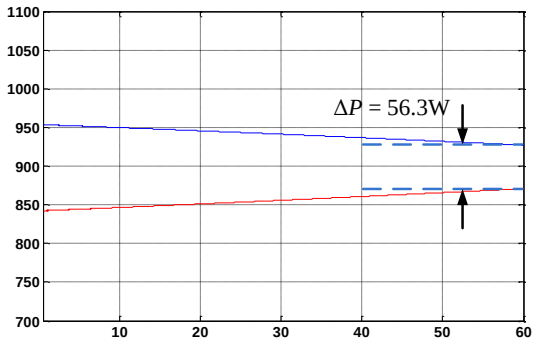

Fig.7. Load power sharing by the SoC-based droop control when n = 2 (Simulation).

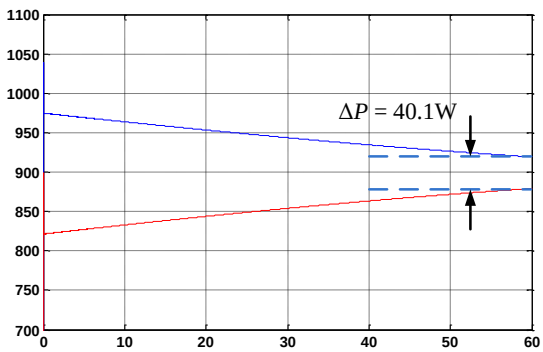

Fig.8. Load power sharing by the SoC-based droop control when n = 3 (Simulation).

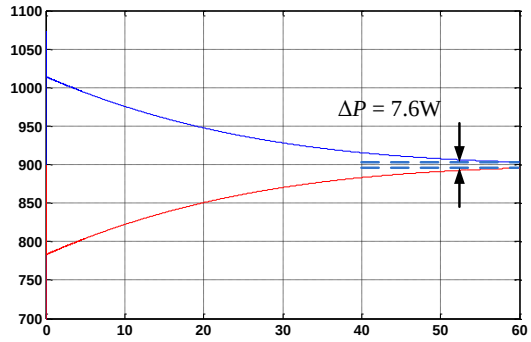

Fig.9. Load power sharing by the SoC-based droop control when n = 6 (Simulation).

IV. EXPERIMENTAL VALIDATION

A 2×2.2 kW prototype of parallel converters is implemented. All the experimental results shown here are sampled by dSPACE 1103. The parameters in the experiment are the same as those in Table I. It should be noticed that for the limitation of the system, the energy storage is virtually implemented in the dSPACE system and SoC of each virtual battery is calculated by (1) and (2).

The proportional load power sharing by droop method is also tested first. As same as that in the simulation, the droop coefficient m_1 is half of m_2. With different droop coefficients, the load power distribution result in the parallel converters is shown in Fig. 10. The data points in Fig. 10 show the experimental results of the output current in each converter. For comparison, the theoretical waveform is also shown. It is seen that the proportional load power sharing is achieved by droop control with different coefficients.

The DC voltage waveform is shown in Fig. 11. The DC voltage deviation is guaranteed to be in the accepted range.

After testing the basic droop function, SoC-based droop method is tested. As same as that in the simulation, the output power waveforms are shown when n equals to 2, 3 and 6, as shown in Fig. 12, Fig. 13 and Fig. 14. It is seen that with larger power exponent n, the load power sharing speed is enhanced. In the experiment, for safe consideration, SoC is not allowed to be lower than 40%.

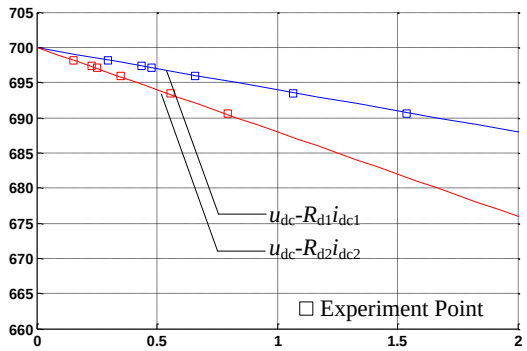

Fig. 10. Results of the proportional power sharing by droop control (Experiment).

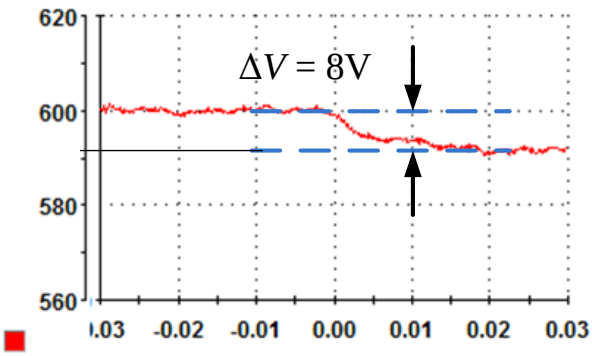

Fig.11. DC voltage deviation caused by droop control (Experiment).

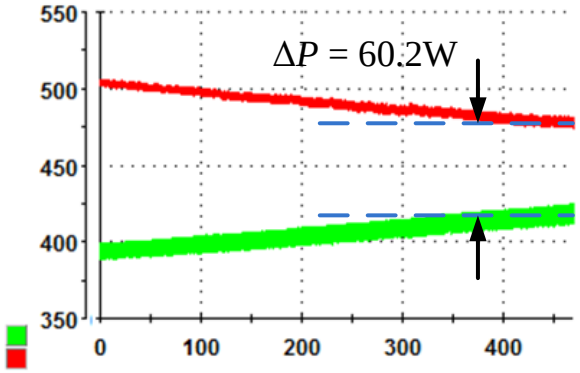

Fig.12. Load power sharing by the SoC-based droop control when n = 2 (Experiment).

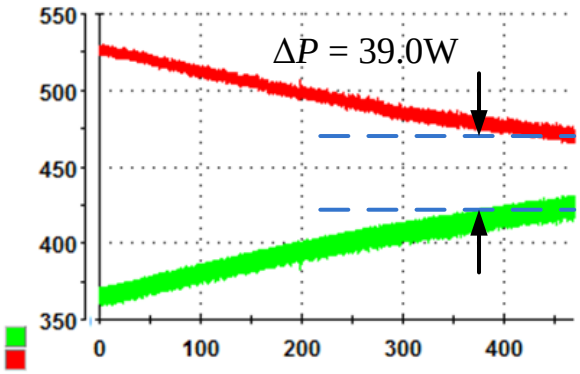

Fig.13. Load power sharing by the SoC-based droop control when n = 3 (Experiment).

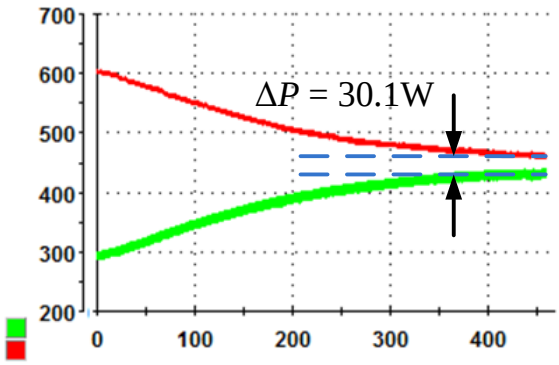

Fig.14. Load power sharing by the SoC-based droop control when n = 6 (Experiment).

V. CONCLUSION

In this paper, a SoC-based droop method is proposed to reach proportional load power sharing in DC distributed energy storage system. With this method, the battery with higher SoC generates more power, while the one with lower SoC generates less power. Different kinds of relationship between SoC and droop coefficient are discussed and the performance of power sharing speed for each relationship is evaluated. It can be tested that with high power exponent of SoC, the power sharing speed is enhanced. Small signal model is realized and system stability is guaranteed. Simulation and experimental results validates the theoretical analysis.

ACKNOWLEDGEMENT

The authors would like to appreciate the financial support by the Power Electronics Science and Education Development Program of Delta Environmental & Educational Foundation (DREG2010007) and also National Natural Science Foundation of China (51177083).

REFERENCES

[1] S. Heier, *Grid Integration of Wind Energy Conversion Systems*. New York: Wiley, 1998.

[2] T. Markvart, *Solar Electricity*, 2nd ed. New York: Wiley, 2000.

[3] R. Lasseter, A. Akhil, C. Marnay, J. Stevens, J. Dagle, etc, "The certs microgrid concept - white paper on integration of distributed energy resources," *Technical Report*, U.S. Department of Energy, April 2002.

[4] J. M. Guerrero, J. C. Vasquez, J. Matas, etc, "Hierarchical control of droop-controlled AC and DC microgrids - a general approach toward standardization," *IEEE Trans. Industrial Electronics*, Vol. 58, No. 1, pp. 158-172, 2011.

[5] Y. Li and Y. W. Li, "Power management of inverter interfaced autonomous microgrid based on virtual frequency-voltage frame," *IEEE Trans. Smart Grid*, Vol. 2, No. 1, pp. 30-40, 2011.

[6] S. Luo, Z. Ye, R.L. Lin, F.C. Lee, "A classification and evaluation of paralleling methods for power supply modules," *in Proc. of PESC*, pp.901-908, 1999.

[7] A.P. Martins, A.S. Carvalho, and A.S. Araújo, "Design and implementation of a current controller for the parallel operation of standard UPSs," *in Proc. of IEEE IECON*, pp.584 ~ 589, 1995.

[8] J. Rajagopalan, K. Xing, Y. Guo and F.C. Lee, "Modeling and dynamic analysis of paralleled dc/dc converters with master-slave current sharing control," *in Proc. of APEC*, pp.678-684, 1996.

[9] T.F. Wu, Y.K. Chen and Y.H. Huang, "3C strategy for inverters in parallel operation achieving an equal current distribution," *IEEE Trans. Industrial Electronics*, Vol.47, No.2, pp.273-281, 2000.

[10] X. Sun, Y.S. Lee and D.H. Xu, "Modeling, Analysis, and Implementation of Parallel Multi-Inverter Systems with Instantaneous Average-Current-Sharing Scheme," *IEEE Trans. Power Electronics*, Vol.18, No.3, pp. 844-856, 2003.

[11] J. M. Guerrero, J. Matas, etc, "Decentralized control for parallel operation of distributed generation inverters using resistive output impedance," *IEEE Trans. Industrial Electronics*, Vol. 54, No. 2, pp. 994-1004, 2007.

[12] J. M. Guerrero, J. C. Vasquez, J. Matas, M. Castilla, etc, "Control strategy for flexible microgrid based on parallel line-interactive UPS systems," *IEEE Trans. Industrial Electronics*, Vol. 56, No. 3, pp. 726-736, 2009.

[13] H. Kakigano, A. Nishino and T. Ise, "Distribution voltage control for DC microgrid with fuzzy control and gain-scheduling control," *in Proc. of ECCE Asia*, pp.256-263, 2011.

[14] Z. Ye, D. Boroyevich, K. Xing, F.C. Lee, "Design of parallel sources in DC distributed power systems by using gain-scheduling technique," *in Proc. of PESC*, pp.161-165, 1999.